Arab J. Nucl. Sci. Appl., Vol. 52, 2, 35-44 (2019)

Arab Journal of Nuclear Sciences and Applications

ISSN 1110-0451 | *Web site: ajnsa.journals.ekb.eg* | (ESNSA)

Investigation of Thermal-Hydraulic Behavior of Supercritical Water Reactor Using Thorium-Uranium Oxide Fuel (ThO_2 - UO_2)

Adel A. Fahmy[1], Adel K. El-Feky[1], Hesham Elkhatib[1], S. Helmy[2, *], Neama M. El-Sahlamy[2]

[1]*Reactors Department, Nuclear Research Center, Atomic Energy Authority (AEA), Cairo, Egypt*

[2]*Nuclear and Radiological Regulatory Authority (NRRA), Cairo, Egypt*

Received 7th June 2018
Accepted 30st Jan. 2019

A Super Critical Water-cooled Nuclear Reactor (SCWR) is a Generation IV concept currently being developed worldwide. Unique to this reactor type is the use of light-water coolant above its critical point. The number of SCWR components is reduced since steam separators and dryers are not required. This advantage drives down capital and maintenance costs. Safety is also increased, because a dry out phenomenon does not occur in SCW conditions; SCW remains in a single phase. A computer program by Engineering Equation Solver, (EES) has been produced for inquiry of the fuel, clad and coolant temperatures under supercritical conditions for supercritical water reactor powered by ThO_2 – UO_2 mixture as a fuel. In the calculation, uniform axial heat flux and average channel were considered. The bulk fluid, clad and fuel temperatures along fuel length were obtained for supercritical pressures 26, 30 and 40 MPa. Also, the UO_2 percentage added to ThO_2 was varied as, 4% and 10%. It was found that the maximum fuel temperature reached 1917 ^{o}C for a pressure of 26 MPa and 1896 ^{o}C for a pressure of 30 MPa in case of 4% UO_2. However, the maximum temperature of the fuel was 1915 ^{o}C for a pressure of 26 MPa and 1894 ^{o}C for a pressure of 30 MPa in case of 10% UO_2, which is surpasses the industry limit of 1850 ^{o}C.

Keywords - (Th, U) O_2 pellets, Thermal conductivity, Thermal hydraulic, Supercritical water reactor

Introduction

Thorium oxide (ThO_2) has recently attracted much attention as a nuclear fuel since it is proliferation resistant and the amount of uranium oxide is limited.

Thorium is not fissile, but can be converted into U-233 which is a fissionable isotope [1]. The behavior of nuclear fuel through irradiation is mainly dependent on its physicochemical properties and their change in temperature and burn-up. Other important thermo-physical properties to be considered are the melting point and density of the fuel. Thorium and uranium oxide fuels utilized in nuclear reactors have very high melting point, but they are of low density and they suffer from poor thermal conductivity [2].

Thermal conductivity of ThO_2 - UO_2 fuel

It is well known that the thermal conductivity of ThO_2 is 50% higher than that of UO_2 over a considerable temperature range [2]. Berman et al. [3] suggested a systematic attempt to correlate thermal conductivity, temperature, and

Corresponding author: *adelalyan@yahoo.com*
DOI: 10.21608/ajnsa.2019.4062.1094

composition for ThO_2 - UO_2system in the early 1970s. Belle and Berman [4] modernized the thermal conductivity correlation to 3126.85 o^C by making use of the enthalpy data.

Melting point

A very important thermo-physical property to be considered for an engineering material, such as nuclear fuel, is the melting point. The onset of melting at the centerline of the fuel rod has been extensively accepted as an upper limit to the allowable thermal rating of nuclear fuel elements [4]. The melting point must be taken into account when considering a new fuel, as it limits the power that can be extracted from the fuel element. The knowledge of the melting point is also important in the fabrication of chemically homogeneous pellets like thoria-urania. ThO_2, and UO_2, have high melting points 3386.85, 2826.85 o^C relatively and they have a low diffusion coefficient at normal sintering temperatures [5].

Figure (1) shows the fuel bundle design with the large diameter center rod, so-called Variant-20 bundle [7], which is used in the current analysis. The central rod has an outside diameter of 20 mm and is assumed to be unheated and the heated length is 5.772 (m). The remaining 42 elements have the outside diameter of 11.5 mm, the hydraulic equivalent diameter of the bundle is 7.83 mm.

MATHEMATICAL MODEL

The following are the recommended equations for the fuel thermal conductivity (K) as a function of temperature (T, K) which are valid from 873 to 1873 (K) for 0%, 4%, 6% and 10%, respectively, of UO_2, [8].

$$K\,[ThO_2] = 1 / (-\,0.03198 + 2.03559 \times 10^{-4} \times T) \quad (1)$$

$$K\,[Th_{0.96}, U_{0.04}]\,O_2 = 1 / (-0.04505 + 2.06241 \times 10^{-4} \times T) \quad (2)$$

$$K\,[Th_{0.94}, U_{0.06}]\,O_2 = 1 / (-0.02884 + 2.6034 \times 10^{-4} \times T) \quad (3)$$

$$K\,[Th_{0.90}, U_{0.10}]\,O_2 = 1 / (-0.04334 + 2.519 \times 10^{-4} \times T) \quad (4)$$

Belle and Berman [4] reported the following equation for the thermal conductivity of 100 % dense ThO_2 in the temperature range of 298-2950 (K),

$$K\,[ThO_2] = (0.0213 + 1.597 \times 10^{-4} \times T)^{-1} \quad (5)$$

Belle and Berman [4] first obtained an expression

for thermal diffusivity up to 2950 (K) as:

$$\alpha[ThO_2]\,(m^2/s) = (-\,34191.1 + 561.28 \times T)^{-1} \quad (6)$$

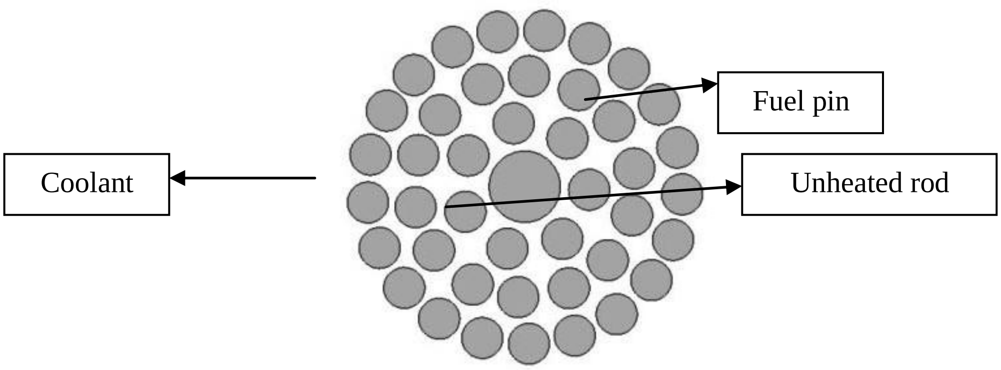

Figure (1): Fuel bundle geometry 43 elements, Variant-20, center element OD 20 mm and the rest – 11.5 mm [6]

Temperature distribution in the axial direction

The following equation represents the power with respect to the axial position or heat-flux ratio:

$$\text{Power ratio} = \dot{q}'_{loc} = \frac{\dot{q}_{loc}}{\dot{q}_{ave}} \quad (7)$$

Where, q_{loc} is local heat flux, W/m^2 and q_{ave} is average heat flux W/m^2

$$\dot{q}_{ave} = \frac{\dot{Q}_{Ch}}{A_h} \quad (8)$$

Where,

$$A_h = \pi l_h \left(N_c D_c + N_{ir} D_{ir} + N_{mr} D_{mr} + N_{or} D_{or}\right) \quad (9)$$

$$\dot{q}'_{loc} = a_0 + a_1 x^1 + a_2 x^2 + a_3 x^3 + a_4 x^4 + a_5 x^5 + a_6 x \quad (10)$$

$$\dot{Q}'_{loc_x} = P_h \int_0^x \dot{q}_{loc} \, dx \quad (11)$$

$$\dot{Q}'_{loc_x} = P_h \, q_{ave} \int_0^x q'_{loc} \, dx \quad (12)$$

$$P_h = \pi \left(N_{ir} D_{ir} + N_{mr} D_{mr} + N_{or} D_{or}\right) \quad (13)$$

$$\int_0^x \dot{q}'_{loc} \, dx = a_0 \frac{1}{1} x + a_1 \frac{1}{2} x^2 + a_2 \frac{1}{3} x^3 + a_3 \frac{1}{4} x^4 + a_4 \frac{1}{5} x^5 + a_5 \frac{1}{6} x^6 + a_6 \frac{1}{7} x \quad (14)$$

The polynomial coefficients ($a_0 - a_6$) are shown in Table (1) [9]

Channel power was calculated through integration of polynomial equation as seen in the following equation:

$$\dot{Q}_{ch} = P_h \, q_{ave} \int_0^{5.772} q'_{loc} \, dx \quad (15)$$

Now Eq. (12) allows calculating the heat output at any axial location. Power per each millimeter increment, along the heated length was calculated by the following equations:

$$\dot{Q}_{loc,mm} = \dot{Q}_{loc,x+1} - \dot{Q}_{loc,x} \quad (16)$$

$$\dot{q}_{loc,x} = \frac{\dot{Q}_{loc,mm}}{A_{mm}} \quad (17)$$

Outer-sheath temperature

The outer - sheath temperature was obtained based on the corresponding bulk-fluid temperature (Tb), i.e., in the same cross section, and HTC. The HTC was calculated according to the Bishop et al. correlation (1964). The correlation of Bishop et al. is suitable for a pressure range from 22.8 to 27.6 MPa, bulk-fluid temperature range − between 282 and 527^{oC}, and heat flux range – between 0.31and 3.46 MW/m^2, which corresponds to the generic SCWR operating conditions [10].

$$Nu_x = 0.0069 \, Re_x \, Pr_x^{0.66} \left(\frac{\rho_w}{\rho_b}\right)_x^{0.43} \left(1 + 2.4 \frac{D_{hy}}{x}\right) \quad (18)$$

The correlation of Swenson et al. was developed using a pressure range of 22.8 – 41.4 MPa, and mass flux of 542 – 2150 kg/m^3. s [11]. The correlation uses the wall temperature to calculate thermo physical properties and is shown in the following equation:

$$Nu_x = 0.00459 \, Re_w^{0.923} Pr_w^{0.613} \left(\frac{\rho_w}{\rho_b}\right)^{0.231} \quad (19)$$

$$D_{hy} = \frac{4A_{flow}}{P_{wetted}} \quad (20)$$

$$A_{flow} = A_{pt} - A_{block} \quad (21)$$

$$P_{wetted} = \pi \left(N_c D_c + N_{ir} D_{ir} + N_{mr} D_{mr} + N_{or} D_{or} + D_{pt}\right) \quad (22)$$

The outer-sheath temperature can be calculated according to the following equation [9].

$$T_{o,sh} = \frac{\dot{q}}{HTC} + T_b \quad (23)$$

Inner-sheath temperature

The inner- sheath temperature can be calculated according to the following equation [9].

$$T_{i,sh} = \frac{\dot{Q}_{sh,x} \ln\left(\frac{r_{o,sh}}{r_{i,sh}}\right)}{2 \pi k_{sh}} + T_{o,sh} \quad (24)$$

Table (1): Polynomial Coefficients for Eqs. 10 -14

Cosine Profile	a_o	a_1	a_2	a_3	a_4	a_5	a_6
Normal	0.0752	0.8888	0.1519	-0.3016	0.1121	0.0182-	1.0758e-3
Upstream	0.0166	1.6104	-0.2439	-0.3484	0.1717	-0.0296	1.7490e-3
Downstream	0.0747	0.7558	0.3514	-0.5203	0.2024	0.0326	1.8439e-3

The correlation of Swenson et al. was developed using a pressure range of 22.8 – 41.4 MPa, and mass flux of 542 – 2150 kg/m^3. s [11]. The correlation uses the wall temperature to calculate thermo physical properties and is shown in the following equation:

$$Nu_x = 0.00459\, Re_w^{0.923} Pr_w^{0.613} \left(\frac{\rho_w}{\rho_b}\right)^{0.231} \quad (19)$$

$$D_{hy} = \frac{4A_{flow}}{P_{wetted}} \quad (20)$$

$$A_{flow} = A_{pt} - A_{block} \quad (21)$$

$$P_{wetted} = \pi \left(N_c D_c + N_{ir} D_{ir} + N_{mr} D_{mr} + N_{or} D_{or} + D_{pt}\right) \quad (22)$$

The outer-sheath temperature can be calculated according to the following equation [9].

$$T_{o,sh} = \frac{\dot{q}}{HTC} + T_b \quad (23)$$

Inner-sheath temperature

The inner- sheath temperature can be calculated according to the following equation [9].

$$T_{i,sh} = \frac{\dot{Q}_{sh,x} \ln\left(\frac{r_{o,sh}}{r_{i,sh}}\right)}{2\,\pi\, k_{sh}} + T_{o,sh} \quad (24)$$

Fuel centerline temperature

The aim of this investigation is to be sure that the fuel ($ThO_2 – UO_2$) centerline temperature (T_b) will be below the industry accepted limit of 1850 ^{o}C. The following correlations were used for the fuel centerline temperature calculations [9]:

$$T_{fc} = \frac{\dot{e}_{gen,mm} \times r_{i,sh}^2}{4\, k_{fuel}} + T_{i,sh} \quad (25)$$

$$\dot{e}_{gen,mm} = \frac{\dot{Q}_{loc,mm}}{D_{i,sh}^2 \times \pi (0.001\, m)} \quad (26)$$

Bulk-fluid temperature

The initial step in the heat-transfer analysis is to determine the bulk-fluid temperature profile along the heated length, which was obtained by the heat-balance method. The inlet bulk-fluid enthalpy (h_x) was obtained based on the inlet temperature of 350°C and constant pressure.

$$h_x = \frac{\dot{Q}_{loc,mm}}{\dot{m}} + h_{x-1} \quad (27)$$

Calculation of the heat transfer coefficient

The Reynolds number is expressed as:

$$Re = \frac{D_{hy} \times v}{\gamma} \quad (28)$$

$$\gamma = \frac{\mu}{\rho} \quad (29)$$

$$Nu_x = \frac{HTC \times D_{hy}}{k_f} \quad (30)$$

Table (2): Selected parameters of proposed SCWR fuel channels. [12,13]

Parameters	Value
Max cladding temperature (design value),	$850^{O}C$
Max fuel centerline temperature (industry accepted limit)	$1850^{O}C$
Heated fuel channel length	5.772 m
Number of fuel rod per bundle	43
Number of heated fuel rods	42
Number of unheated fuel rods	1
Diameter of heated fuel rods (# of rods)	11.5 (35) & 13.5 (8) mm
Diameter of unheated fuel rod	20 mm
Hydraulic equivalent diameter of fuel channel	7.83 mm
Heated area of fuel channel	$8.76m^2$
Flow area of fuel channel	$3729mm^2$

Results

In this part, a summary of the results of the steady state calculation of the fuel, clad and coolant temperatures are given. The bulk fluid, clad and fuel temperatures along fuel length were obtained for supercritical pressures 24, 30 and 40 MPa. Also, the UO_2 percentage added to ThO_2 was varied, 4% and 10%.

Figure (2) Shows the fuel centerline temperature of thorium-uranium oxide fuel containing 4% UO_2 for different supercritical pressures. It is clear that the temperature surpasses the industry limit of 1850 °C. The fuel centerline temperature decreases with increasing the supercritical temperature due to increasing in the heat transfer coefficient reaching to the values 7419, 8157, and 10474 kW/m2 °C associated with the supercritical pressures 26, 30 and 40 MPa respectively.

Figure (3) depicts the clad temperature distribution at different supercritical pressures for the fuel containing 4% UO_2. The maximum clad temperature reaches to 848, 797.3 and 688.3°C which is associated with the supercritical pressures of 26, 30 and 40 MPa respectively. The clad temperature decrease is due to the increase of the heat transfer coefficient with increasing of supercritical pressures.

Figure (4) illustrates the relation of the reactor coolant temperature with the heated length of the fuel for different supercritical pressures. The coolant temperature decreases with the increase of the supercritical pressure due to the increase of coolant specific heat, The maximum outlet temperature reaches 609.9, 577.7 and 512 ^{O}C at 26, 30 and 40 MPa respectively.

Figure (5) shows the fuel centerline temperature at 10% UO_2, for different supercritical pressures, where it is clear that the temperature surpasses the industry limit of 1850 ^{O}C. The fuel centerline temperature decreases with increasing the supercritical temperature due to increasing in the heat transfer coefficient, as seen in Figure (5), but in this case the maximum fuel temperatures are lower than the maximum fuel temperature in case of 4% UO_2, due to increasing of fuel conductivity.

For 10% UO_2, fuel, Figure (6) describes the clad temperature distribution at different supercritical pressures. The clad temperature decreasing is due to increasing of the heat transfer coefficient with increasing of supercritical pressures.

Figure (7) reavels the effect of the supercritical pressure on the reactor coolant temperature along the heated length of the fuel. The coolant temperature found decreases with increases of the supercritical pressure due to increasing of coolant specific heat.

Figure (8) shows that there is a good match between the present work and that reported by Lisa Grande et al. [9] for fuel clad and coolant temperatures, and shows that both of fuel temperature curves surpass the industry limit which is 1850 °C and that the clad temperature is about to touch the clad temperature limit which is 850 °C. It is also noticed that the clad temperature for the present work at any heated length is higher than that early reported [9], where the fuel clad materials used is Inconel-600, whereas model 304 st-steel was used as a cladding material in the present investigation model. It is known that the thermal conductivity of the Inconel-600 is higher than that of SS-304.

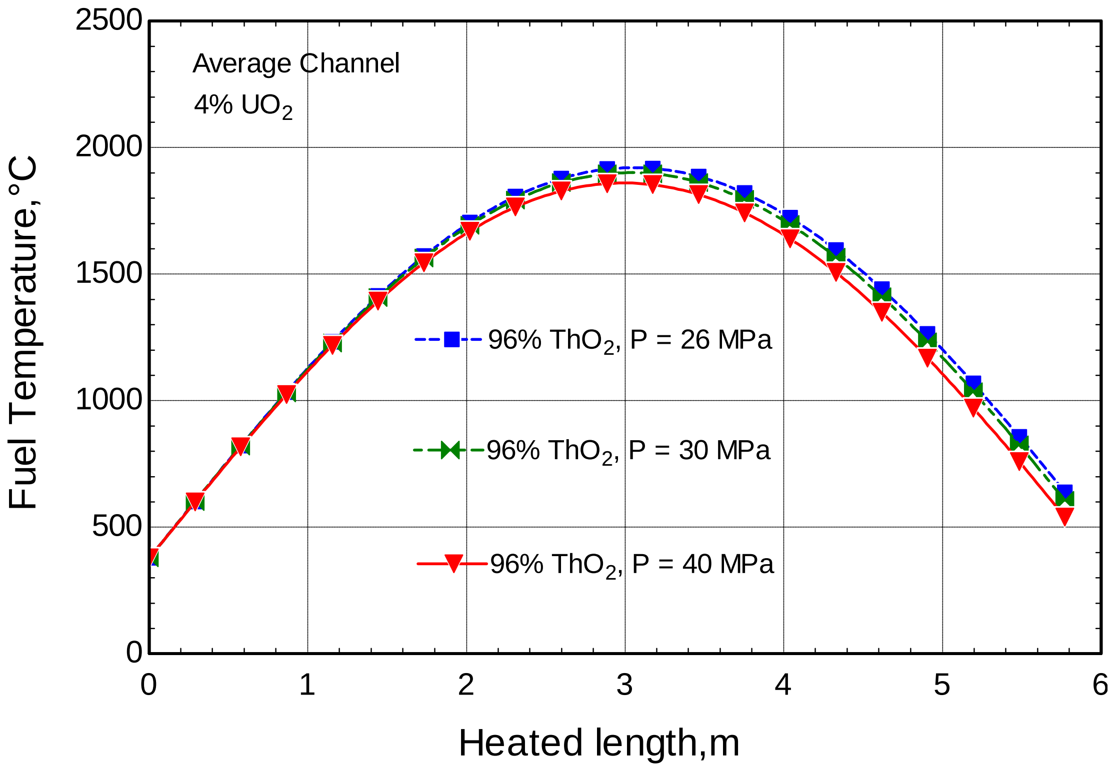

Figure (2): Fuel temperature distribution at 4% UO_2 for different supercritical pressures

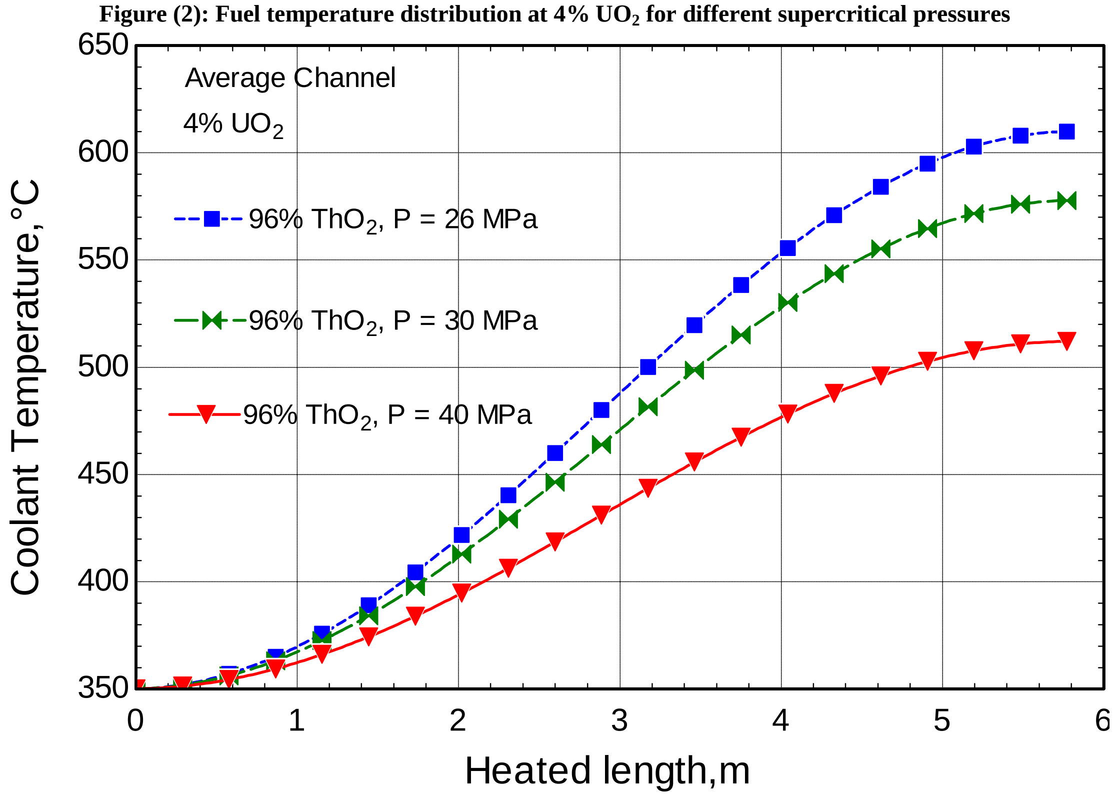

Figure (3): Clad temperature distribution at 4% UO_2 for different supercritical pressures

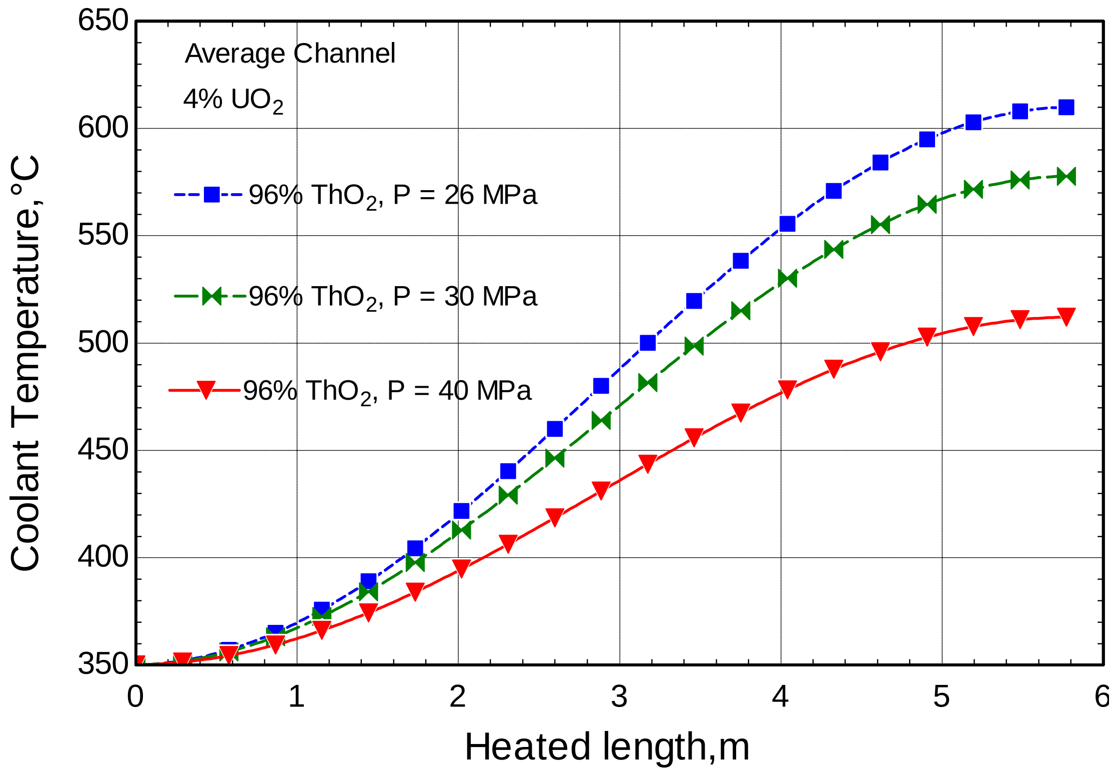

Figure (4): Coolant temperature distribution at 4% UO_2 for different supercritical pressures

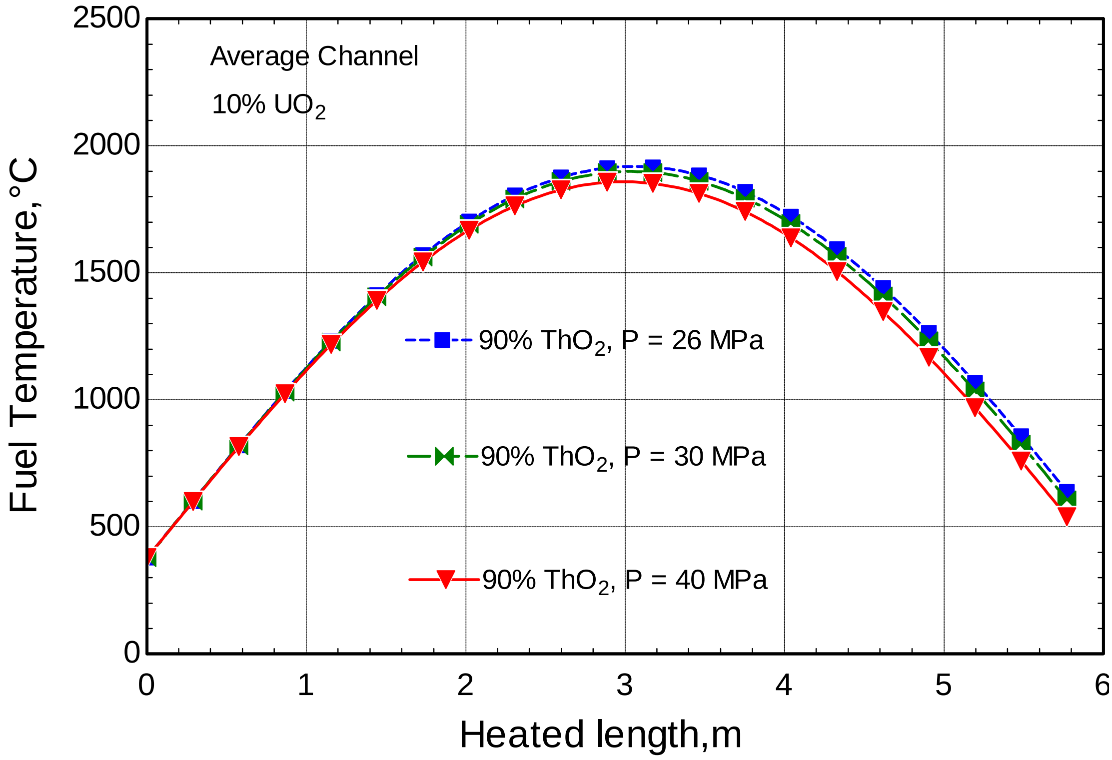

Figure (5): Fuel temperature distribution at 10% UO_2 for different supercritical pressures

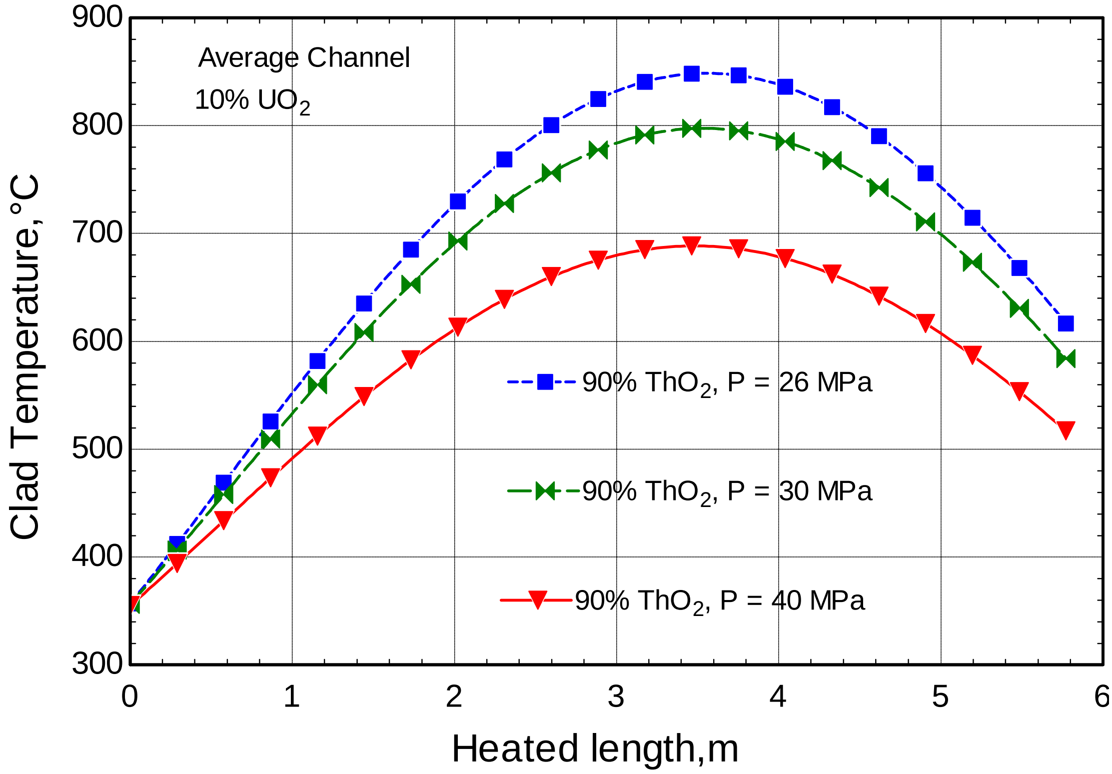

Figure (6): Clad temperature distribution at 10% UO_2 for different supercritical pressures

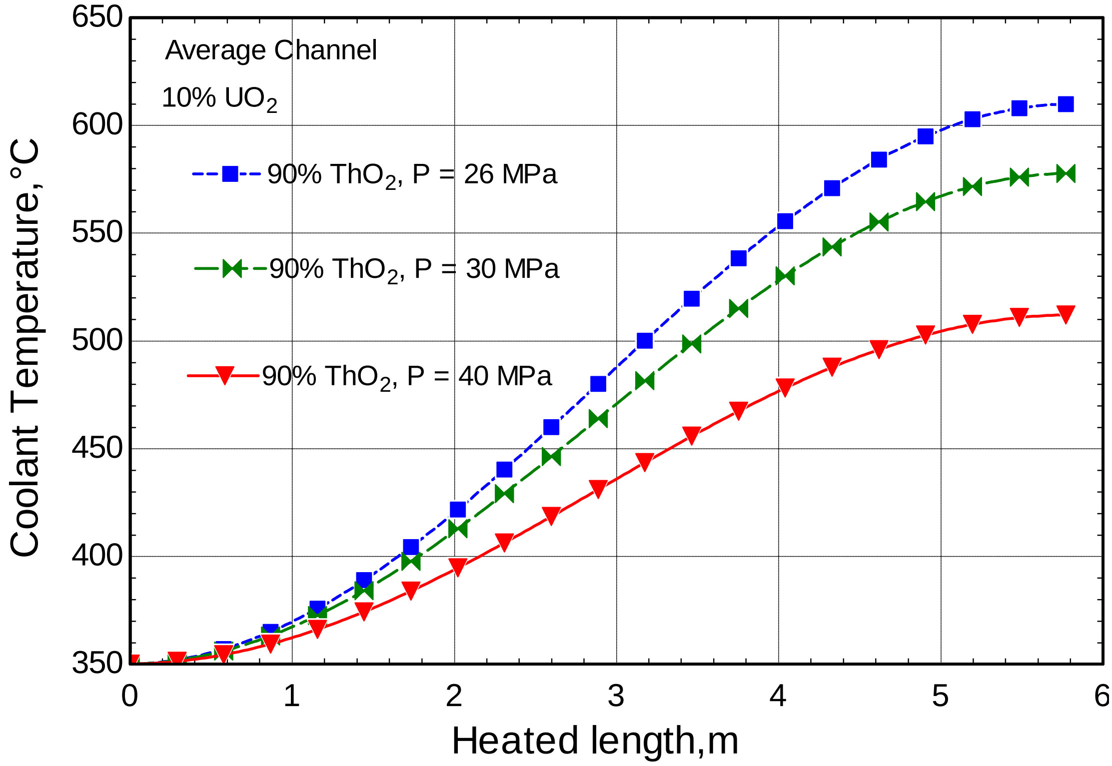

Figure (7): Coolant temperature distribution at 10% UO_2 for different supercritical pressures

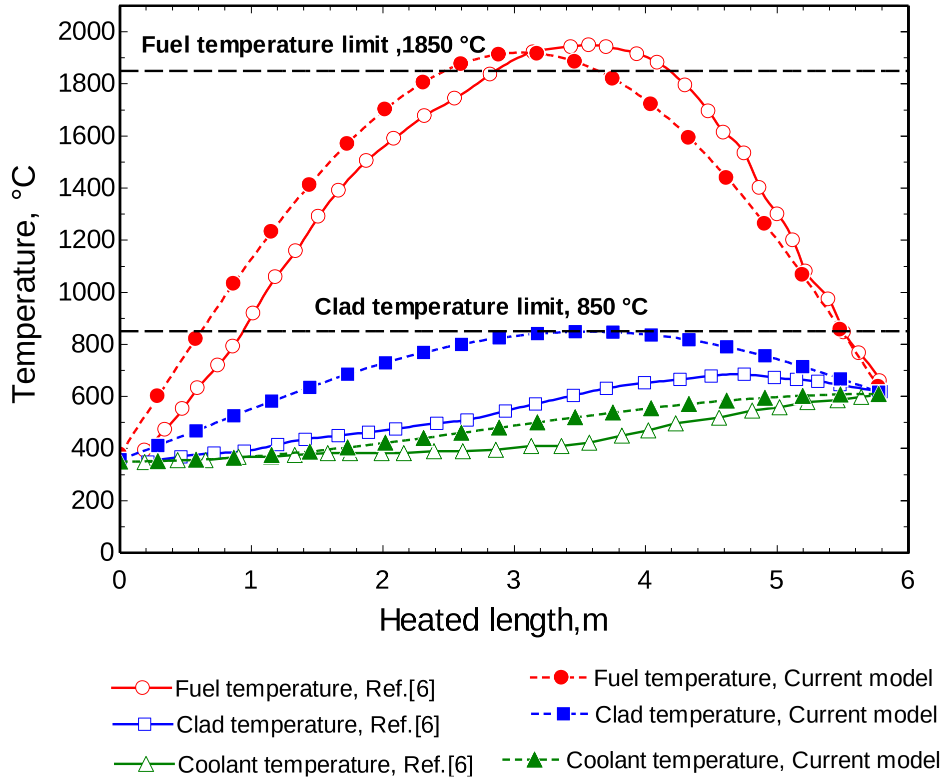

Figure (8): Comparison between the present work, Ref. [6]

Conclusion

For the investigated variable parameters, the fuel centerline temperature surpassed the industry limit temperature, which is 1850 °C in case of 4% UO_2 and 10% UO_2 for all supercritical pressures. The clad temperature also exceeded the clad industry limit which is 850 °C. However, on the other hand, as the supercritical pressure increased, the fuel, clad and coolant temperatures have been found to decrease. Adding of UO_2 to the thoria, resulted in a high fuel temperature exceeding the industry limit. Hence using UO_2 as a nuclear fuel might not be the correct choice for supercritical water-cooled reactors (SCWRs). Thoria has also a high melting point which is very important in terms of fuel failures and release of fission product, this high melting point increases the durability and safety during normal and abnormal reactor operations. Using Inconel-600 seems to be the best sheath material choice compared to 304 st-steel because of its higher mechanical strength at high pressures and temperatures.

Nomenclature

a_i	Polynomial coefficient.
A	area, m^2.
A_{flow}	flow area, m^2.
C_p	specific heat capacity at a given pressure, J/kg. K.
HTC	Heat Transfer Coefficient, W/m^2. K.
D	diameter, m.
h	enthalpy, J/kg.
$\dot{e}_{gen}$	volumetric heat flux, W/m3.
k	thermal conductivity, W/m K.
l	length, m.
$\dot{m}$	mass-flow rate, kg/s.
Nu	Nusselt number, dimensionless.
p	perimeter, m.
P	pressure, Pa.
Pr	Prandtl number, dimensionless.
Q	heat transfer, J.
$\dot{Q}$	heat transfer rate, W.
$\dot{q}$	heat flux, W/m2.
$\dot{q}'$	power ratio.
r	radius, m.
Re	Reynolds number, dimensionless.
T	temperature, ^{O}C.
SCWR	Super Critical Water Reactor.

Greek Symbols

μ	dynamic viscosity, Pa· s.
ν	kinematic viscosity, m^2/s.
ρ	density, kg/m^3.

Subscripts

ave	average.
b	bulk.
block	cross sectional area blocking fluid flow.
c	center.
Ch	channel.
fc	fuel centerline.
flow	cross sectional flow area.
fuel	fuel.
hy	hydraulic equivalent.
i	inner.
ir	inner ring.
loc	local.
mm	per millimeter increment.
o	outer.
or	outer ring.
pt	pressure tube.
sh	sheath.
w	wall.
wetted	wetted.
x	axial location along heated length.

References

1- Ki Won Kang, Jae Ho Yang, Keon Sik Kim, Kun Woo Song, Chan Bock Lee, and Youn Ho Jung,"(Th,U) O2 Pellets : Fabrication and Thermal Properties," Journal of the Korean Nuclear Society,(35)299 – 308,(2003).

2- T. R. GovindanKutty, Joydipta Banerjee and Arun Kumar, "Thermophysical Properties of Thoria-based Fuels," Springer International Publishing AG, London, 11-70, (2013)

3- Berman RM, Tully TS, Bell J, Goldberg I., "The thermal conductivity of polycrystalline thoria and thoria-urania solution,"LMWR Development Program WAPD-TM-908, (1972);https://inis.iaea.org/search/search.aspx?orig_q=RN:4063316

4- Belle J, Berman RM, "Thorium dioxide: properties and nuclear applications," Naval Reactors Office, United State Department of Energy,(1984);https://inis.iaea.org/search/search.aspx?orig_q=RN:16071971

5- Olson GL, McCardell RK, Illum DB, Fuel summary report: "shippingport light water breeder reactor" Idaho National Engineering and Environmental Laboratory Report INEEL/EXT-98-00799 Rev.1, 1999;

https://inis.iaea.org/search/search.aspx?orig_q=RN:32028722

6- Liza Christine Grande, "Thermal Aspects of Using Alternative Nuclear Fuels in Supercritical Water-Cooled Reactors, "Master Thesis, Institute of Technology, Ontario University, 2010.

7- Leung, L., "Effect of CANDU bundle geometry variation on dryout power," Proc.of ICONE Conf. 16. Paper #48827, p.8. Orlando, Florida, USA: ASME,2008.

8- Thermo physical Properties database of materials for light water reactors and heavy water reactors, International Atomic Energy Agency, Vienna, Austria (2005).

9- Lisa Grande, Bryan Villamere, Adrianexy Rodriguez-Prado, Sally Mikhael, Leyland Allison and Igor Pioro.,"Some Thermal Aspects of Using Thoria Fuel in SuperCritical Water-Cooled Nuclear Reactors,"Proc. of the 17th International Conf. of Nuclear Engineering ICONE17. Brussels, Belgium,July 12-16,2009.

10- Bishop, A., Sandberg, R., & Tong, L.,"Forced convection heat transfer to water at near-critical temperatures and super-critical pressures," Atomic Power Division. Pittsburgh, PA, USA: Westinghouse Electric Corporation, (1964).

11- H.S. Swenson, J.R. Carver, and C.R. Kakarala.,"Heat transfer to supercritical water in smooth-bore tubes, Journal of Heat Transfer," 87 (4) (1965).

12- Naidin, M., Mokry, S., Pioro, I., Duffey, R., and Zirn, "U. SCW NPPs: Layouts and Thermodynamic Cycles," Proc. of Int. Conf. of Nuclear Energy for New Europe, Bled, Slovenia, Sep. 14-17, 2009.

13- Eugene Saltanov., " Steam-Reheat Option for Supercritical Water Cooled Reactors. Ontario," Ontario Univ; 2010.